Research Article

Ching Ching Lam and Kendall N. Houk*

Exploring reaction dynamics involving post-transition state bifurcations based on quantum mechanical ambimodal transition states

https://doi.org/10.1515/pac-2025-0462
Received March 18, 2025; accepted April 4, 2025

Abstract: Computational methods for predicting product ratios in dynamically controlled reactions with shallow intermediates or bifurcating pathways after an ambimodal transition state are reviewed and benchmarked. The range of methods includes molecular dynamics simulations, machine learning-based models and recent advancements in correlational methods, all of which rely on quantum mechanical computations. Together, these approaches form a computational toolbox that enhances the efficiency and effectiveness of exploring reaction selectivity influenced by dynamic effects.

Keywords: Ambimodal transition state; quantum mechanics (QM); quantum science and technology; reaction dynamics effects; selectivity predictions.

Introduction

The development of quantum mechanical methods and computers over the last century has made it possible to study the intricacies of mechanisms even for highly complex reactions. When considering reaction selectivity, most chemists immediately think of kinetic effects or transition state theory (TST). According to TST, the reaction pathway with the lowest activation barrier is the most favorable and leads to the major product (Fig. 1A). In some cases, reaction dynamic effects can also play a significant role. These reactions typically feature a bifurcating potential energy surface (PES) with a valley-ridge inflection (VRI) point (Fig. 1B) or a shallow entropic intermediate (Fig. 1C) following an ambimodal transition state (TS) leading to multiple pathways. [1]

The concept of reaction dynamic effects was once considered a rare phenomenon. Carpenter, the pioneer of organic dynamics, was one of the first to highlight instances where statistical kinetic models failed in predicting the outcomes of organic reactions.[2] His work on temperature-dependent stereoselectivity in the thermal isomerization of bicyclo[2.1.1]hexene-5-dis from 1984 is considered a landmark in the field.[3] The concept of post-transition state bifurcations was then introduced. A review by Houk et al. summarized many foundational studies on post-transition state bifurcations.[4] One of the most noteworthy examples is the work from the research group of Ruedenberg, a giant in the field of quantum mechanics (QM), on the ring opening of cyclopropylidene to allene stereoisomers.[5] The reaction is one of the first reported examples of a bifurcating process in the literature

Article note: A collection of invited papers to celebrate the UN's proclamation of 2025 as the International Year of Quantum Science and Technology.

***Corresponding author: Kendall N. Houk**, Department of Chemistry and Biochemistry, University of California Los Angeles, Los Angeles, CA 90095-1569, USA, E-mail: houk@chem.ucla.edu. https://orcid.org/0000-0002-8387-5261
Ching Ching Lam, Department of Chemistry and Biochemistry, University of California Los Angeles, Los Angeles, CA 90095-1569, USA. https://orcid.org/0000-0001-7332-5656

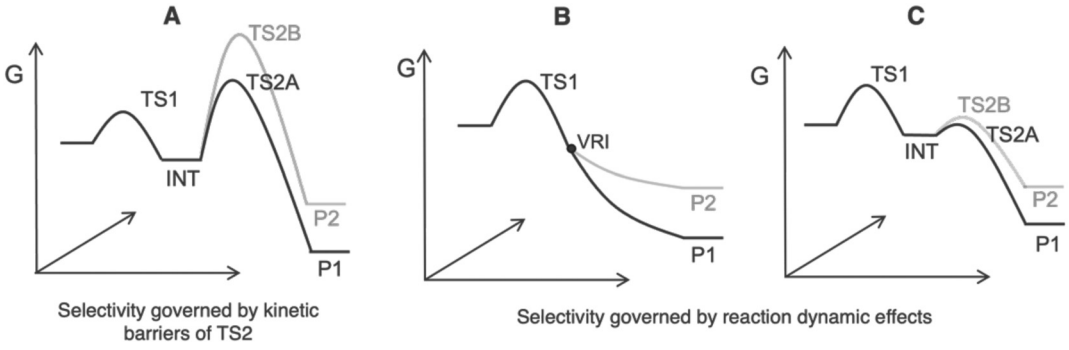

Fig. 1: Typical energy profiles in chemical reactions. VRI = valley-ridge inflection point.

(Fig. 2A). Another significant set of works comes from Caramella et al. They used quantum mechanical computations to investigate bifurcating pathways in the dimerization of various common organic motifs, including butadiene, cyclopentadiene, and cyclopentadienone.[6,13,14] Taking the dimerization of cyclopentadiene as an example, this reaction exhibits a bifurcating pathway that leads to two possible but identical Diels–Alder adducts (Fig. 2B). Beyond theoretical concepts, the work from Houk and Snapper et al. represents one of the early experimental and computational collaborative efforts in investigating reaction dynamics (Fig. 2C). The study focused on the intramolecular cycloadditions of cyclobutadiene with dienes. The [4 + 2] and [2 + 2] adducts compete dynamically in this reaction.[7]

In the past 20 years, the scope of reactions governed by reaction dynamic effects has expanded significantly. Advancements in computational technology enable the exploration of increasingly complex chemical systems. Ongoing research continues to highlight the role of quantum mechanical calculations in predicting reaction dynamics and controlling selectivity. The Beckmann reactions studied by Yamataka et al. are examples (Fig. 2D).[8,15] Pathways from the ambimodal TS led to either fragmentation or rearranged products. Computations using QM showed that the selectivity is influenced by electronic substituent effects. Likewise, Bogle and Singleton et al.,[9] in their computational study on the nucleophilic substitution of dichlorovinyl ketone (Fig. 2E), found that the selectivity of bifurcating reactions can be strongly affected by the activated vibrational mode in the ambimodal transition state. Beyond organic reactions, there are also a growing number of reports on dynamically controlled organometallic reactions. An early study from Houk et al. involves bifurcating Diels–Alder/hetero-Diels–Alder reactions (Fig. 2F). Additions of Lewis acid catalysts like $SnCl_4$ and $BiCl_3$ can reverse selectivity, favoring the hetero-Diels–Alder pathway.[16] Transition metal-catalyzed reactions can also exhibit bifurcating selectivity. For example, the gold(I)-catalyzed homo-Rautenstrauch rearrangement studied by Nevado et al. features a bifurcating PES that leads to either a 1,2- or 1,3-carboxylate migration product (Fig. 2G).[10] Another classic example comes from Davis et al. on rhodium(II)-catalyzed reactions, which display dynamically competing pathways to either C–H activation/Cope rearrangement (CHCR) or direct C–H insertion (Fig. 2H).[11] Notably, dynamic effects are not limited to synthetic chemistry but also play a crucial role in biosynthetically relevant systems. For example, from the work of Tantillo et al., the selectivity outcome in the carbocation isomerization process in the biosynthesis of terpene natural products is found to be influenced by dynamic effects. [17–19]

Recognizing the growing impact of reaction dynamics, several comprehensive reviews have summarized key developments and trends in terms of the scope of the dynamically controlled chemical reactions. The review in 2017[20] and the book chapter in 2021[21] from Tantillo et al. provides a comprehensive overview of recent developments in the field. Ess also highlighted the significance of reaction dynamic effects in studies of organometallic reactions in an account from 2021.[22] Goodman et al.[23–25] have also compiled a dataset of dynamically controlled chemical reactions from the literature up to 2019.

Computations have become ever more essential in unravelling reaction mechanisms, with calculating energy profiles using density functional theory (DFT) now a standard approach for investigating selectivity. Energy profiles pinpoint key saddle points, including ground and transition states, on the PES. For reactions governed by dynamic effects, energy profiles alone cannot fully explain reactivity. Often, for these reactions, the selectivity

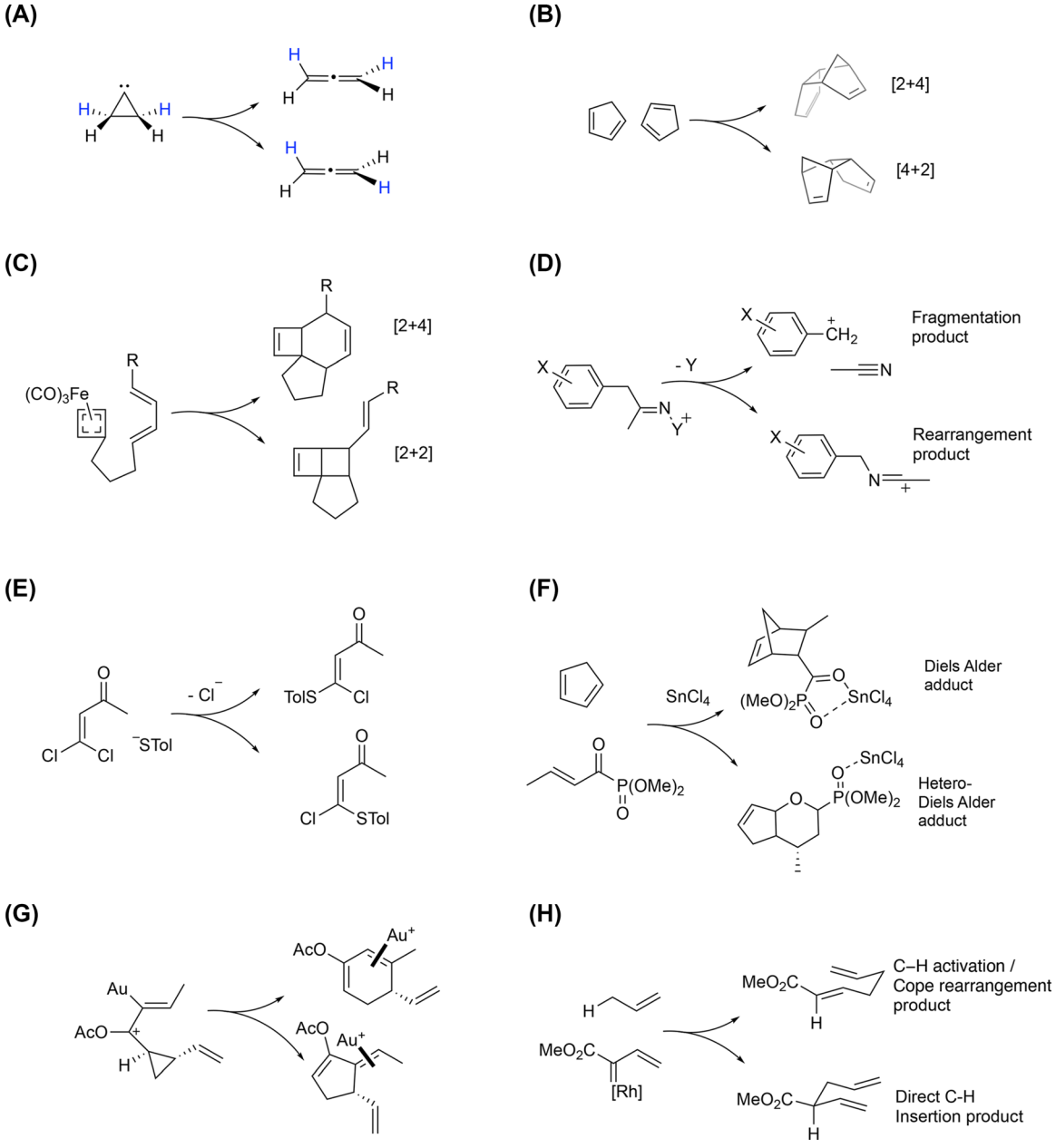

Fig. 2: Examples of bifurcating reactions from the literature. Reaction dynamic effects play important roles in directing selectivity in a variety of different reactions.[5–12] (A) Ring opening of cyclopropylidene (Ruedenberg et al.). (B) Dimerization of cyclopentadiene (Caramella et al.). (C) Cycloadditions of cyclobutadiene with dienes (Houk and Snapper et al.). (D) Bifurcation in the Beckmann reactions (Yamataka et al.). (E) Nucleophilic substitution to dichlorovinyl ketone (Bogle and Singleton et al.). (F) Lewis acid catalysed Hetero-Diels-Alder/Diels-Alder reactions (Houk et al.). (G) Au-catalyzed homo-Rautenstrauch rearrangement (Nevado et al.). (H) Rh-catalyzed C–H functionalization (Davies et al.).

calculated from the kinetic barriers does not match experiments and the energy profile exhibits features suggestive of an ambimodal TS or a shallow intermediate. At this point, chemists should often consider reaction dynamics effects, moving beyond the conventional assumptions of TST.[21]

This review provides an overview of computational methods for investigating reaction dynamic effects includes post-transition state bifurcations and predicting selectivity after establishing the energy profile (Fig. 3). The review begins with a discussion of molecular dynamics (MD) simulations incorporating QM. Recent advancements in machine learning-based methods are then elaborated, where data from quantum mechanical

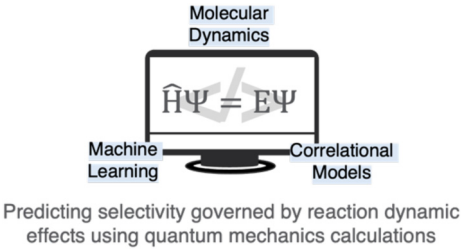

Fig. 3: A graphic summary of this review: molecular dynamics simulations, machine learning-based models and recent advancements in correlational methods are discussed below.

calculations are used for training. Correlational models are subsequently explored and benchmarked. These models allow rapid predictions based solely on standard DFT calculations.

Molecular dynamics simulations

Quasi-classical dynamic (QCD) simulations

Quasi-classical dynamic (QCD) simulations are widely employed to investigate reaction mechanisms.[26] For nearly all reactions discussed in the introduction, QCD simulations were performed as part of the research to predict product ratios and confirm dynamic effects. Over the years, several software programs have been developed to facilitate QCD simulations in conjunction with electronic structure programs, such as Gaussian,[27] which perform the required QM calculations. Examples include VENUS from Hase et al.,[28–30] the open-source program Progdyn from Singleton et al.[31,32] and Ess' Milo program,[33,34] which was written in Python.

QCD simulations generate trajectories that describe the time evolution of the reacting system and predict possible reaction outcomes. QCD trajectories are typically initiated from the TS structure via random sampling from zero-point energy and thermal energy contributions of molecular vibrational modes.[34] This part of the calculations is considered at the QM level, usually with DFT. The propagation of QCD trajectories is based on classical mechanics. The velocity Verlet algorithm,[35] a numerical integration method for propagating trajectories based on Newton's equations of motion, is commonly used for trajectory propagation in QCD simulations and has been implemented in both Progdyn and Milo.

To accurately determine the selectivity outcomes of a dynamically controlled reaction, the QCD simulation process needs to be repeated from the ambimodal TS, generating tens to hundreds of trajectories to obtain a reliable product ratio.[36] Most QCD trajectories in organic reaction studies are generated using a step size of 1 femtosecond (fs).[22] Depending on the chemical system, a complete QCD trajectory from the TS to the product can range from a few hundred to several thousand fs. Thus, performing QCD simulations at a reasonable level of theory using DFT functionals remains computationally expensive at the time of writing this report, particularly for large chemical systems.

Quantum mechanics/molecular mechanics (QM/MM) treatments

Molecular dynamics simulations using the hybrid quantum mechanics/molecular mechanics (QM/MM) approach offer a powerful solution for studying reaction dynamics beyond systems involving only the reacting substrate.[37,38] In QM/MM simulations, the reactive fragments are typically treated at the quantum mechanical level, like in the QCD simulation, in terms of electronic structure and frequency calculations, while the surrounding environment is modelled using molecular mechanics force fields.

QM/MM approach is particularly useful for studying enzymatic reactions.[39] The biosynthesis of terpene natural products, an example of reaction dynamic effects in nature mentioned in the introduction of this paper, has been studied at the QM/MM level by Major et al. to account for the influence of the enzymatic environment (Fig. 4A).[40] Another example is in the study of the enzymatic [4 + 2]/[6 + 4] bifurcating reaction with pericyclase

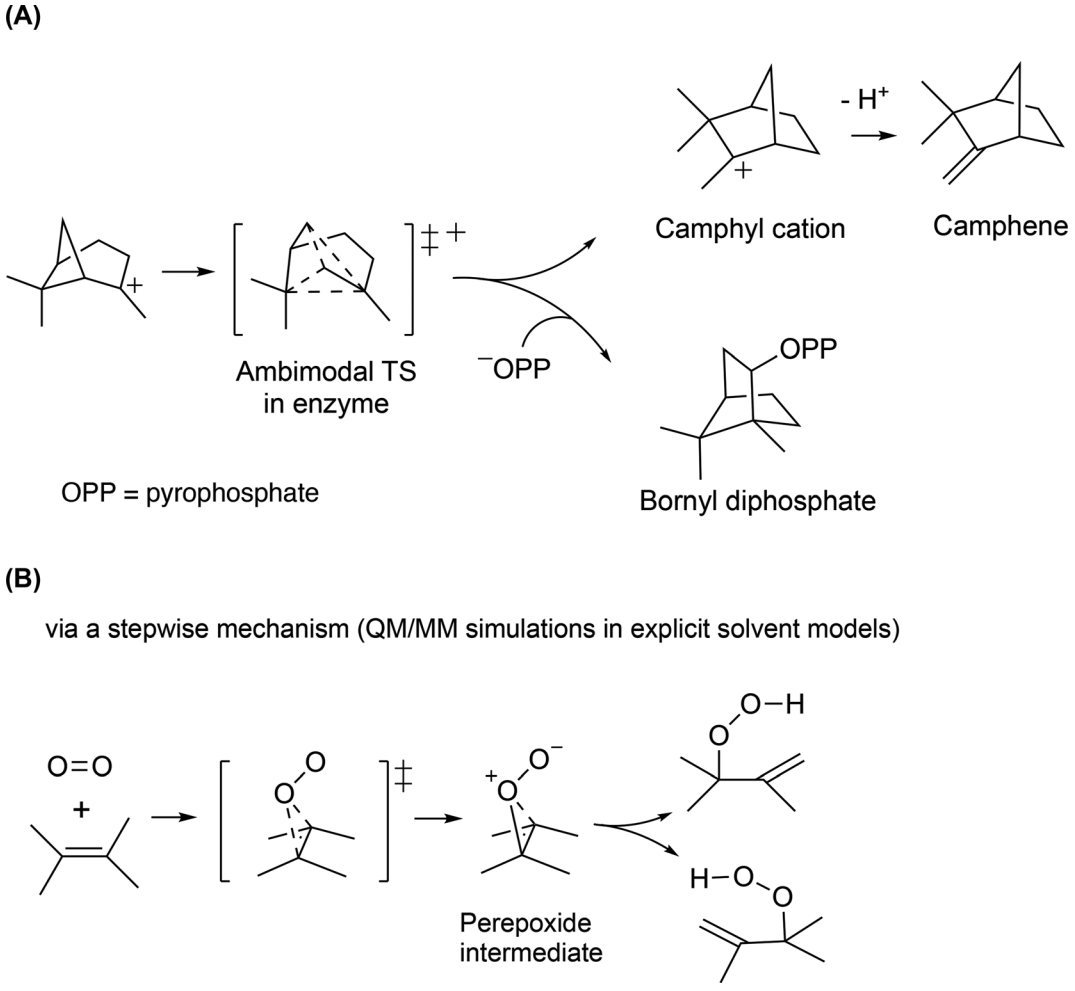

Fig. 4: Representative examples of dynamically controlled reactions studied using a QM/MM approach.[40,41] (A) Biosynthetic carbocation rearrangement reaction (Major et al.). (B) Ene reaction between singlet oxygen and alkene (Acevedo et al.).

SpnF (Fig. 6D) from Houk et al.[42] They developed the environment-perturbed transition-state sampling (EPTSS) method, which employed calculations with QM/MM to calculate barriers of TSs. Calculations revealed that the reaction proceeded through a single [4 + 2]/[6 + 4] ambimodal transition state under enzymatic conditions. The [4 + 2] to [6 + 4] adduct ratio is 11:1 in the enzyme compared to 1.6:1 in the aqueous condition.

Solvent effects sometimes play a critical role, necessitating the inclusion of an explicit solvent model. The QM/MM approach can effectively address this. An example is the bifurcating ene reactions between singlet molecular oxygen and tetramethyl ethylene from investigations conducted by Acevedo et al. (Fig. 4B).[41] Their QM/MM studies with an explicit solvent model revealed a traditional stepwise mechanism, in contrast to the concerted mechanism observed in the gas phase.

Explorations on machine learning approaches

QCD trajectories from simulations and TS analyses at the QM level generate large amounts of data about the reaction channels and the bifurcating PES of a chemical system. Recently, attempts have been made to utilize these data with machine learning (ML) approaches[43–45] to train models for predicting selectivity outcomes of bifurcating reactions.

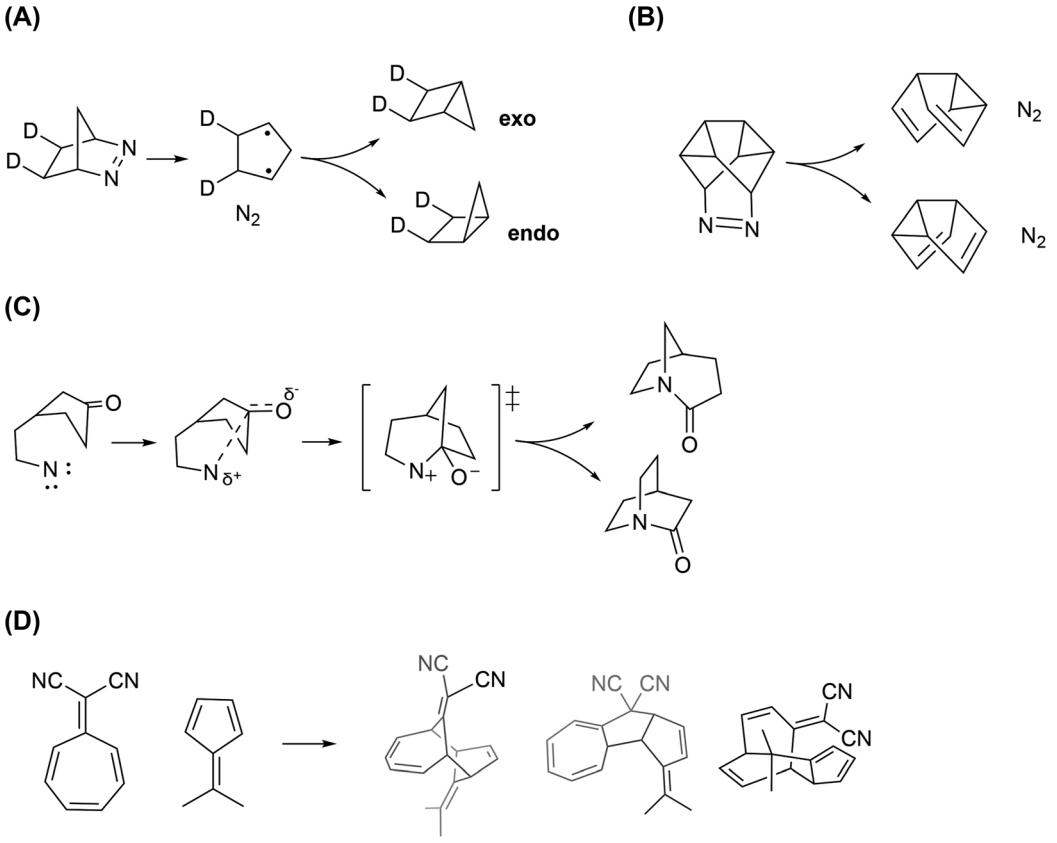

Fig. 5: Examples of reactions modelled using a machine learning approach to predict the major product, using data from QCD trajectories and transition state analyses at the QM level.[46,48–52] (A) Thermal deazetization (Ess et al.). (B) N_2 extrusion reactions (Ess et al.). (C) Schmidt–Aubé reaction (Tantillo and Hsu et al.). (D) Tripericyclic reaction (Houk and Gómez-Bombarelli et al.).

One approach is extracting physical parameters from the reaction trajectories and the bifurcating TS as descriptors for training classifier models, such as the random forest and logistic regressor, to predict the major product. Ess et al. have explored this approach in a study on thermal deazetization of 2,3-diazabicyclo[2.2.1]hept-2-ene, a reaction that proceeds through a shallow intermediate (Fig. 5A).[46,47] This intermediate gives rise to two dynamically competing pathways, leading to the *endo* or *exo* product. Their analysis demonstrates that energy and vibrational mode parameters from the TS structure alone are insufficient for accurately predicting trajectory outcomes. Incorporating atomic velocities and positions from QCD trajectories enhances the performance of classifier models. In a simpler chemical system, where selectivity is governed by the motion of two competing bonds, a ML model built using ambimodal TS features has achieved good accuracy. Ess et al. showcased this in their study[48] on cyclopentadienone dimerization from Caramella et al.[13] and N_2 extrusion reactions (Fig. 5B).[53] Here, mass-weighted displacements (MWD) and velocities (MWV) from frequency analyses of the TS are key features in predicting the major product. Takayanagi et al. also investigated a group of [4 + 2]/[2 + 2] bifurcating cycloadditions between cyclobutadiene and butadiene with classifier models. Their features importance analyses also come to a similar conclusion.[54] MWD and MWV features contribute significantly to the accuracy of the model.

ML approaches can also be used to improve simulation methodologies and enhance efficiency. One of the bottlenecks of running QCD simulations is performing the integration to obtain the atomic force for trajectory propagation. Hsu et al.[49] addressed this challenge by training a kernel ridge regression (KRR) model using data from QCD simulations of Schmidt–Aubé reactions (Fig. 5C).[50] The KRR model was trained on Coulomb matrices, derived from molecular geometries in QCD trajectories, as descriptors. By replacing the velocity Verlet algorithm in Progdyn, the KRR can efficiently propagate trajectory steps, significantly enhancing computational speed by 100-fold. Alternatively, Gómez-Bombarelli et al.[51] proposed an active learning pipeline that employs a graph

convolutional neural network model to generate reaction-specific ML potentials using DFT data. Generating trajectories using ML potentials is 2000 times faster than running traditional quasi-classical MD simulations. They further adopted a transfer learning approach to account for the solvent and enhance the accuracy of the ML potentials, applying it to evaluate solvent effects in the tripericyclic reactions studied by Houk et al. (Fig. 5D) [52]

Correlational models

In recent years, several correlational models have been developed to enable rapid predictions of product ratios in bifurcating reactions using only data from stand-alone DFT calculations based on structural coordinates obtained from optimizations and frequency analyses.

The following sections provide an overview of several methodologies in chronological order of their publication: the bond length difference (dBond) method introduced by Houk et al.,[55] the VRAI-selectivity approach developed by Goodman et al.,[23–25] the reactive mode composition factor (RMCF) analysis proposed by Srnec et al.,[56] and the structural difference (dRMSD) method (2023), also from Houk et al.[57]

We have now conducted a benchmarking study to evaluate the performance of these models. We used data from Yang et al.,[58] who performed quasi-classical dynamic simulations on four examples of [4 + 2]/[6 + 4] bifurcating reactions at the B3LYP-D3/6-31G(d) level of theory.[59–61] Specifically, these four reactions are diene/triene cycloaddition (DTA), tethered-diene/triene cycloaddition (DTB), NgnD-catalyzed reaction (NgnD) and SpnF-catalyzed reaction (SpnF) (Fig. 6). The procedure and results of this benchmarking study will be presented alongside the overview of these methodologies to provide a comprehensive evaluation of the model performance. The results of the benchmarking study are presented in Table 1. We have written Python scripts to automate the product ratio calculation on top of the existing published scripts from Goodman and Srnec et al. See the supporting information for details of the code.

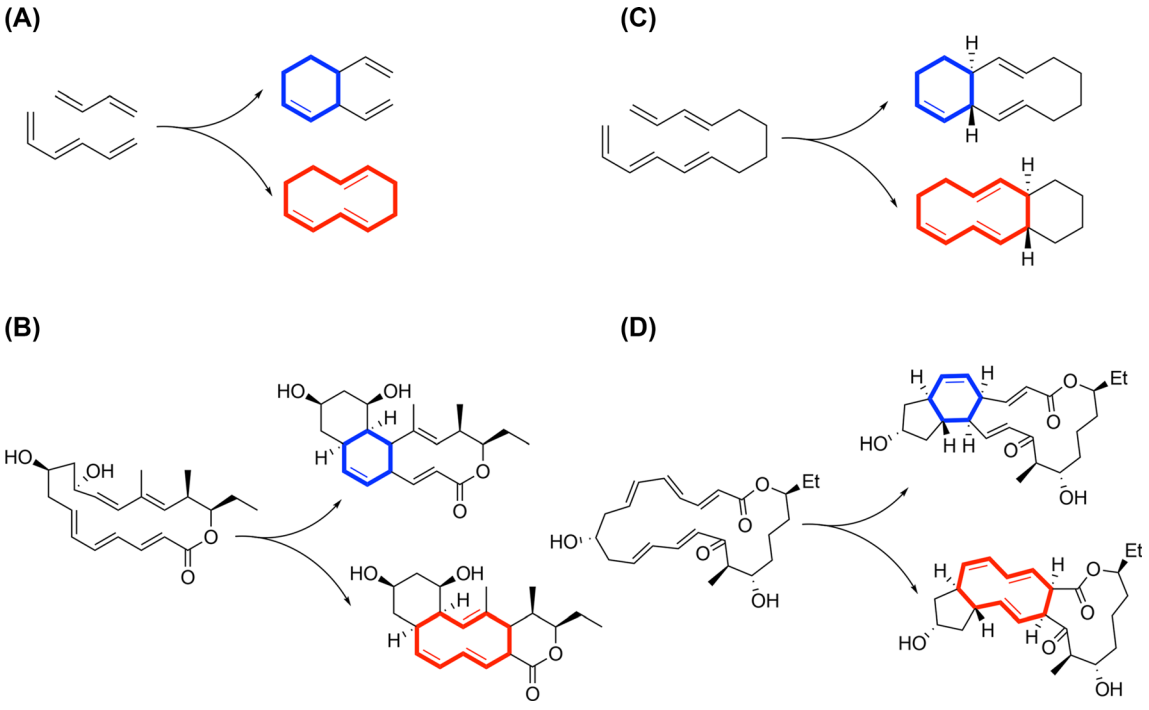

Fig. 6: Reactions in the [4 + 2]/[6 + 4] bifurcating reaction dataset from Yang et al.[58] (A) Diene/Triene Cycloaddition (DTA). (B) NgnD-Catalyzed Diels-Alder Reaction. (C) Tethered-Diene/Triene Cycloaddition (DTB). (D) SpnF-Catalyzed Diels-Alder Reaction.

Table 1: Benchmarking on correlational models. This table compares the predicted [4 + 2] and [6 + 4] product percentages from correlation models to results from QCD simulations.

	QCD prediction[58]		dBond[55]		VRAI-selectivity[23–25]		RMCF analysis[56]		dRMSD[57]	
	[4 + 2]	[6 + 4]	[4 + 2]	[6 + 4]	[4 + 2]	[6 + 4]	[4 + 2]	[6 + 4]	[4 + 2]	[6 + 4]
DTA	79 %	21 %	89 %	11 %	95 %	5 %	88 %	12 %	15 %	85 %
DTB	33 %	67 %	32 %	68 %	34 %	66 %	62 %	38 %	44 %	56 %
NgnD	24 %	76 %	18 %	82 %	17 %	83 %	63 %	37 %	46 %	54 %
SpnF	52 %	48 %	33 %	67 %	25 %	75 %	77 %	23 %	67 %	33 %

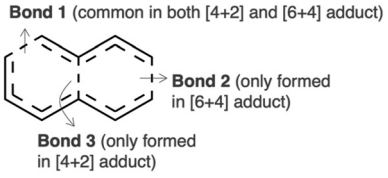

Fig. 7: Key bond parameters (Bond 1, Bond 2 and Bond 3) in the dBond model using the ambimodal TS of reaction DTA (Fig. 6A) as an example.

Bond length difference (dBond) method

The dBond method is derived from a study investigating the relationship between product ratios and the atomic distances of forming bonds in ambimodal pericyclic reactions.[55] The study is based on a dataset of 15 reactions, all of which share common features. In these reactions, two possible products, referred to as Product A and Product B, are formed in dynamic competitions. The corresponding ambimodal TS structure features three potential-forming bonds: Bond 1, Bond 2 and Bond 3. Among these, Bond 1 is consistently present in both products, while Bond 2 forms exclusively in Product A and Bond 3 forms only in Product B. Fig. 7 takes reaction DTA as an example and highlights the specific locations of Bond 1, 2 and 3 in the TS structure of the reaction. Through statistical analyses, a linear correlation was derived (eq. (1)):

$$\ln(B:A) = -9.3\,(L_{\mathrm{Bond3}} - L_{\mathrm{Bond2}}) \tag{1}$$

B:*A* is the product ratio of Product B to Product A. L_{bond3} and L_{bond2} are the bond length of Bond 2 and Bond 3, respectively.

In the benchmarking study, we wrote and applied a script, dBond.py (see SI), to perform the analyses outlined by Houk et al. automatically. Eq. (1) was used to compute the [4 + 2] to [6 + 4] product ratio. The dBond procedure predicts the correct selectivity for three out of four cases. In the case of SpnF, the dBond method predicts 1:2 instead of the QCD ratio of 1:1. While the predicted product ratios showed good agreement with the results from QCD simulations, it is important to note that reactions DTA, DTB, and SpnF were included in the original dataset used to develop this method.

VRAI-selectivity

The VRAI-selectivity program from Goodman et al. is a fully automated Python program for predicting selectivity outcomes in dynamically controlled reactions. The algorithm was first developed to address bifurcating reactions featuring a VRI point (Fig. 1B)[24] and then modified to extend its applicability to dynamically controlled reactions that involve a shallow intermediate (Fig. 1C).[23]

VRAI-selectivity algorithm takes the geometries and frequency of the TS1, TS^{II} and products as inputs. In bifurcating reactions with a VRI point, TS1 is the ambimodal TS and TS^{II} is the TS that connects product 1 and product 2 (P1 and P2). In the scenario of a reaction with a shallow intermediate, VRAI-selectivity takes the geometry of the intermediate as input instead of TS^{II}. VRAI-selectivity reduces the PES to two dimensions by considering the bond difference between TS1 and the products (Fig. 8). The major product is identified based on

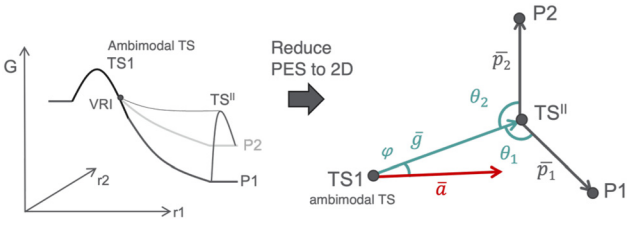

Fig. 8: Illustrating the VRAI-selectivity algorithm. $\bar{a}$ is the imaginary eigenvector of TS1. $\bar{g}$ is the displacement between TS1 and TS^{II}. TS^{II} are connected to P1 and P2 via vector $\overline{p_1}$ and $\overline{p_2}$. In the case of a [4 + 2]/[6 + 4] bifurcating reaction, TS^{II} is the cope rearrangement reaction that converts the [6 + 4] to [4 + 2] adduct.

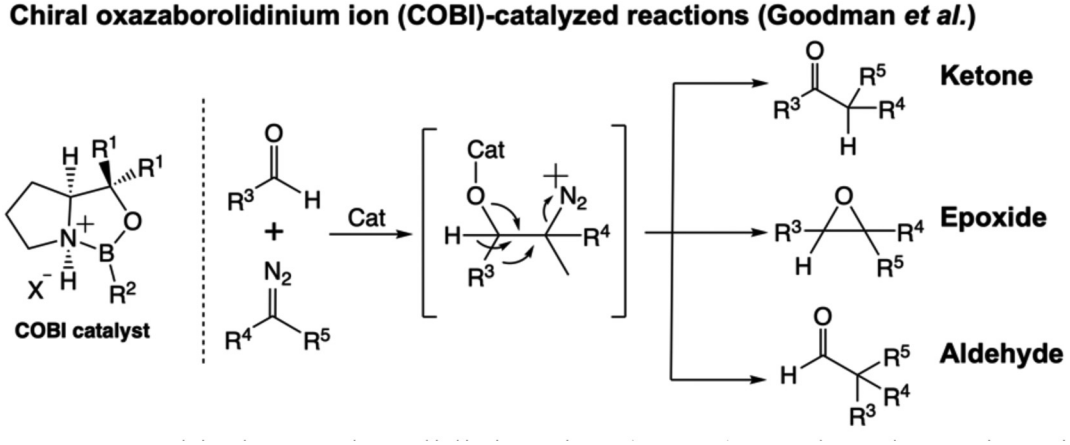

Fig. 9: Chiral oxazaborolidinium ion (COBI)-catalyzed reactions in the study from Goodman et al.[25] VRAI-selectivity accounts for both stereo- and chemoselectivity outcomes of the reactions, which are controlled by reaction dynamics.

the direction of the TS1 imaginary eigenvector, $\bar{a}$, relative to the intermediate or TS2 on the PES. The product ratio is calculated by estimating the width of the bifurcating valley using harmonic oscillator approximation with frequency analysis results on TS1. VRAI-multi,[25] a Python extension of VRAI-selectivity, streamlines and automates product percentage calculations when more than two products arise from the ambimodal TS.

VRAI-selectivity was developed using a dataset of approximately 60 reactions, consisting of a wide range of organic reactions, collected from the literature published between 2003 and 2019. In 2023, Goodman et al. demonstrated the effectiveness of the program on a set of complex organic reactions catalyzed by chiral oxazaborolidinium ion (COBI) catalysts (Fig. 9).[25,62] These chemical systems exhibit significant complexity, ranging from 90 to 112 atoms. For systems of this scale, studying them using the traditional approach of quasi-classical simulations was computationally infeasible due to the high cost. The study demonstrates that transition state theory alone cannot explain the selectivity outcome. The use of VRAI-selectivity confirms that selectivity is heavily influenced by reaction dynamics.

In the benchmarking study, we used the VRAI-selectivity Python scripts and outputs from DFT calculations to compute the product ratio of the [4 + 2]/[6 + 4] bifurcating reactions. VRAI-selectivity correctly predicted the major product in three out of four reactions. The prediction on SpnF again deviates from the QCD result 1:1, giving 1:3 instead. Notably, there is no overlap between the four reactions in the benchmarking dataset and the dataset used for developing VRAI-selectivity.

Reactive mode composition factor (RMCF) analysis

The RMCF analysis method[56] of Srnec et al. predicts the selectivity of bifurcating reactions by calculating the atomic kinetic energy distribution (KED) factors using the frequency analysis output of the ambimodal TS. $KED_{j\alpha}$ represents the fraction of the kinetic energy associated with atom j within the reactive mode (α), *i.e.* the imaginary frequency mode (eq. (2)).

$$\mathrm{KED}_{j\alpha} = \left(\frac{m_j r_j^2}{\sum_k m_k r_k^2} \right)_{j\alpha} \tag{2}$$

m_j is the mass of atom j and r_j is the atomic displacement of atom j in reactive mode α. $\sum_k m_k r_k^2$ is the mass-weighted squared displacement of all atoms in the system. Based on eq. (2), low-mass atoms with large displacement in the reactive mode tend to have a higher $\mathrm{KED}_{j\alpha}$.

In a bifurcating reaction leading to two possible products, A and B, two different groups of atoms are involved in bond formation and dissociation in each reaction channel. Excluding the bonds that are commonly formed or broken, these sets of atoms are designated as Partition A and Partition B. The product ratio of the bifurcating reaction is computed by calculating the ratio of KED_A to KED_B. KED_A and KED_B are the sum of atomic KED factors within Partition A and B, respectively. In cases with more than two products from the ambimodal TS, additional partitions can be defined using the same approach and accounted for in calculating the product ratio.

Srnec et al. have developed a Python script (rmcf.py), which we have utilized to compute atomic KED factors.[56] Referring to Fig. 7 on the dBond analysis process, Bond 2 and Bond 3 are identified from the ambimodal TS for each reaction. Atoms in Bond 2 were assigned to Partition A, while atoms in Bond 3 were assigned to Partition B. The RMCF method successfully predicted the major product of DTA and SpnF reaction in our benchmarking dataset. For DTB and NgnD, RMCF analyses overestimate the product percentage of [4 + 2] adducts,

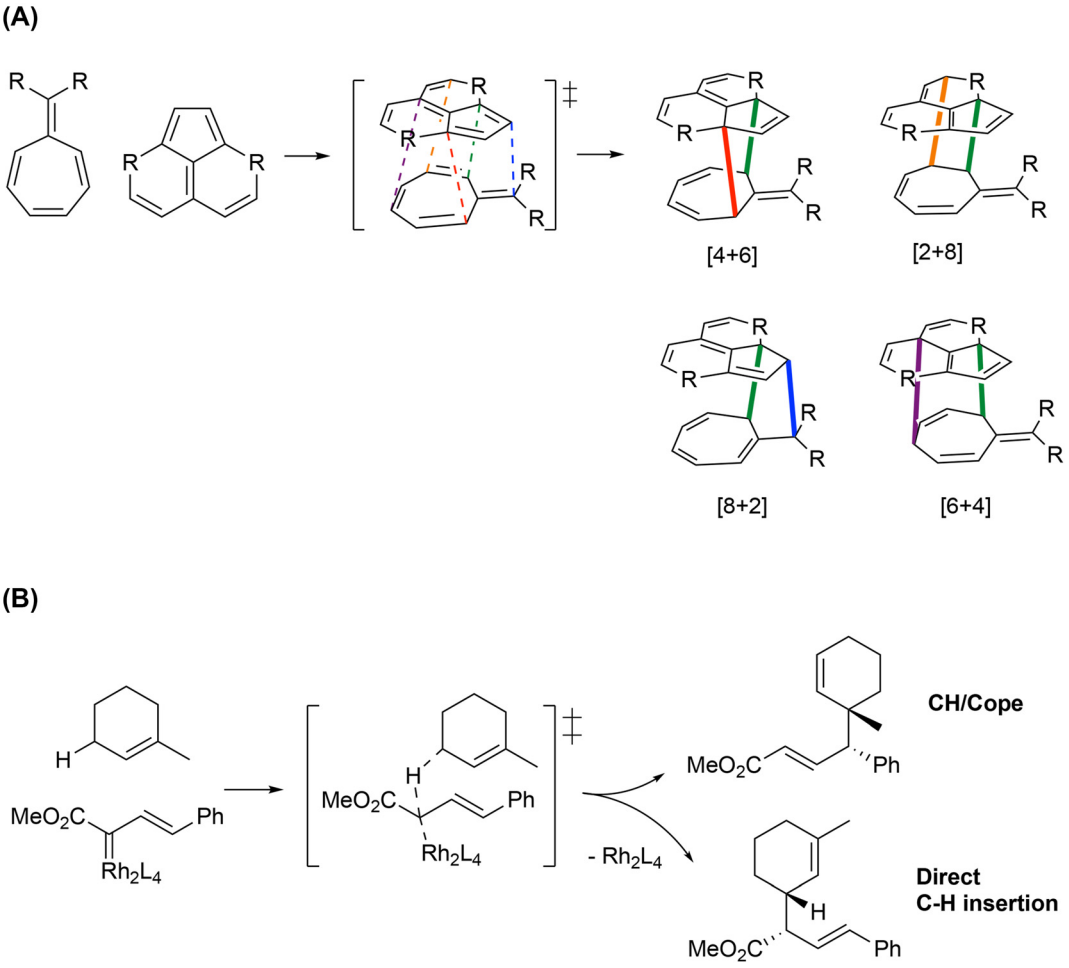

Fig. 10: The structural difference (dRMSD) method is generalized based on the above reactions.[57,63] (A) Tetrapericyclic cycloaddition reaction (Houk et al.). (B) C–H functionalization/Cope rearrangement bifurcating reaction (Davies, Yang and Houk et al.).

predicting over 60 % compared to approximately 30 % in QCD simulations. RMCF analyses also did not reproduce the rough 1:1 ratio from QCD simulations of SpnF.

Structural difference (dRMSD) method

The structural difference (dRMSD) method was initiated by Houk et al. as a generalization during their study of a tetrapericyclic cycloaddition reaction (Fig. 10A). [57] Houk et al. identified a strong negative linear correlation (correlation coefficient = –0.981) between the root mean square deviation (RMSD) of the ambimodal TS relative to the product structure and the corresponding product percentage obtained from quasi-classical dynamic simulations. In 2024, Davies, Yang and Houk et al. demonstrated that this correlation between RMSD and product ratio is also applicable to a group of C–H functionalization/Cope rearrangement bifurcating reactions (Fig. 10B), with the trend holding for three out of four cases.[63]

In the benchmarking study of [4 + 2]/[6 + 4] bifurcating reactions, we calculated the RMSD of the ambimodal transition state (TS) to each product, predicting the major product as the one with the lower RMSD value. For consistency in comparison with other correlational methods, the product percentage was calculated using eq. (3).

$$P_A = \frac{1/\mathrm{RMSD}_A}{\sum_j 1/\mathrm{RMSD}_j} \times 100\,\% \tag{3}$$

P_A is the product percentage for product A and RMSD_A represents RMSD between the ambimodal TS to product A. $\sum_j \mathrm{RMSD}_j$ denotes the total RMSD measurements of the ambimodal TS to its products. This equation also applies to cases when there are more than two products from the ambimodal TS, such as the tripericyclic and tetrapericyclic cycloaddition reaction.[57] The dRMSD method successfully predicts the major product for two out of four cases and the predicted ratio noticeably deviates from the QCD methods.

Conclusions

This review summarizes computational tools available to chemists for predicting the product ratio of dynamically controlled reactions. We have covered molecular dynamic simulations, models using machine learning approaches and innovative developments in correlational methods. These advancements enable faster predictions of reaction selectivity and help confirm reaction dynamic effects more efficiently. A benchmarking study was conducted to compare the correlation models for the [4 + 2]/[6 + 4] bifurcating reaction dataset.

When selectivity predictions based on transition state theory do not align with experimental results, even after thorough benchmarking and conformational exploration, it will always be valuable to explore the role of dynamic effects. Correlational models, given the speed and minimal computational requirements, offer a valuable starting point for rapid estimations of selectivity from an ambimodal TS. Molecular dynamics simulations can then provide deeper insights into the reaction mechanism and provide a more accurate prediction of the reaction selectivity. By integrating these approaches, a more complete and accurate understanding of selectivity influenced by reaction dynamic effects can be achieved.

Acknowledgments: C.C.L. thanks Croucher Foundation and the Croucher Postdoctoral Fellowship program for the financial support of this project. K.N.H. thanks the National Science Foundation (CHE2153972) for financial support. This work used computational and storage services associated with the Hoffman2 Shared Cluster provided by the UCLA Institute for Digital Research and Education's Research Technology Group.
Research ethics: Not applicable.
Informed consent: Not applicable.

Author contributions: All authors have accepted responsibility for the entire content of this manuscript and approved its submission. C. C. Lam performed the research and wrote the paper with the guidance of Prof. K. N. Houk. Prof. K. N. Houk conceptualized and supervised the project.
Use of Large Language Models, AI and Machine Learning Tools: ChatGPT for checking grammar and polishing text.
Conflict of interest: The authors state no conflict of interest.
Research funding: Croucher Postdoctoral Fellowship from Croucher Foundation National Science Foundation (CHE-2153972).
Data availability: All the data for this paper is available on GitHub: github.com/chingchinglam71/bifucating_product_ratio_prediction.

References

1. Rehbein, J.; Carpenter, B. K. Do We Fully Understand What Controls Chemical Selectivity? *Phys. Chem. Chem. Phys.* **2011**, *13* (47), 20906–20922. https://doi.org/10.1039/C1CP22565K.
2. Carpenter, B. K. Intramolecular Dynamics for the Organic Chemist. *Acc. Chem. Res*. **1992**, *25* (11), 520–528. https://doi.org/10.1021/ar00023a006.
3. Newman-Evans, R. H.; Carpenter, B. K. Temperature Dependence of Stereoselectivity as a Criterion for Mechanism. Rearrangement of Bicyclo[2.1.1]Hexene-5-d and Two Phenyl Derivatives. *J. Am. Chem. Soc*. **1984**, *106* (25), 7994–7995. https://doi.org/10.1021/ja00337a070.
4. Ess, D. H.; Wheeler, S. E.; Iafe, R. G.; Xu, L.; Çelebi-Ölçüm, N.; Houk, K. N. Bifurcations on Potential Energy Surfaces of Organic Reactions. *Angew. Chem., Int. Ed.* **2008**, *47* (40), 7592–7601. https://doi.org/10.1002/anie.200800918.
5. Valtazanos, P.; Elbert, S. T.; Xantheas, S.; Ruedenberg, K. The Ring Opening of Cyclopropylidene to Allene: Global Features of the Reaction Surface. *Theor. Chim. Acta* **1991**, *78* (5), 287–326. https://doi.org/10.1007/BF01112344.
6. Caramella, P.; Quadrelli, P.; Toma, L. An Unexpected Bispericyclic Transition Structure Leading to 4+2 and 2+4 Cycloadducts in the Endo Dimerization of Cyclopentadiene. *J. Am. Chem. Soc*. **2002**, *124* (7), 1130–1131. https://doi.org/10.1021/ja016622h.
7. Limanto, J.; Khuong, K. S.; Houk, K. N.; Snapper, M. L. Intramolecular Cycloadditions of Cyclobutadiene with Dienes: Experimental and Computational Studies of the Competing (2 + 2) and (4 + 2) Modes of Reaction. *J. Am. Chem. Soc*. **2003**, *125* (52), 16310–16321. https://doi.org/10.1021/ja0380547.
8. Yamamoto, Y.; Hasegawa, H.; Yamataka, H. Dynamic Path Bifurcation in the Beckmann Reaction: Support from Kinetic Analyses. *J. Org. Chem*. **2011**, *76* (11), 4652–4660. https://doi.org/10.1021/jo200728t.
9. Bogle, X. S.; Singleton, D. A. Dynamic Origin of the Stereoselectivity of a Nucleophilic Substitution Reaction. *Org. Lett*. **2012**, *14* (10), 2528–2531. https://doi.org/10.1021/ol300817a.
10. Garayalde, D.; Gómez-Bengoa, E.; Huang, X.; Goeke, A.; Nevado, C. Mechanistic Insights in Gold-Stabilized Nonclassical Carbocations: Gold-Catalyzed Rearrangement of 3-Cyclopropyl Propargylic Acetates. *J. Am. Chem. Soc*. **2010**, *132* (13), 4720–4730. https://doi.org/10.1021/ja909013j.
11. Hansen, J. H.; Gregg, T. M.; Ovalles, S. R.; Lian, Y.; Autschbach, J.; Davies, H. M. L. On the Mechanism and Selectivity of the Combined C−H Activation/Cope Rearrangement. *J. Am. Chem. Soc*. **2011**, *133* (13), 5076–5085. https://doi.org/10.1021/ja111408v.
12. Çelebi-Ölçüm, N.; Ess, D. H.; Aviyente, V.; Houk, K. N. Effect of Lewis Acid Catalysts on Diels–Alder and Hetero-Diels–Alder Cycloadditions Sharing a Common Transition State. *J. Org. Chem*. **2008**, *73* (19), 7472–7480. https://doi.org/10.1021/jo801076t.
13. Quadrelli, P.; Romano, S.; Toma, L.; Caramella, P. A Bispericyclic Transition Structure Allows for Efficient Relief of Antiaromaticity Enhancing Reactivity and Endo Stereoselectivity in the Dimerization of the Fleeting Cyclopentadienone. *J. Org. Chem*. **2003**, *68* (15), 6035–6038. https://doi.org/10.1021/jo034401j.
14. Quadrelli, P.; Romano, S.; Toma, L.; Caramella, P. Merging and Bifurcation of 4+2 and 2+4 Cycloaddition Modes in the Archetypal Dimerization of Butadiene. A Case of Competing Bispericyclic, Pericyclic and Diradical Paths. *Tetrahedron Lett*. **2002**, *43* (48), 8785–8789. https://doi.org/10.1016/S0040-4039(02)02014-2.
15. Katori, T.; Itoh, S.; Sato, M.; Yamataka, H. Reaction Pathways and Possible Path Bifurcation for the Schmidt Reaction. *J. Am. Chem. Soc*. **2010**, *132* (10), 3413–3422. https://doi.org/10.1021/ja908899u.
16. Çelebi-Ölçüm, N.; Ess, D. H.; Aviyente, V.; Houk, K. N. Lewis Acid Catalysis Alters the Shapes and Products of Bis-Pericyclic Diels–Alder Transition States. *J. Am. Chem. Soc*. **2007**, *129* (15), 4528–4529. https://doi.org/10.1021/ja070686w.
17. Hong, Y. J.; Tantillo, D. J. Biosynthetic Consequences of Multiple Sequential Post-Transition-State Bifurcations. *Nat. Chem*. **2014**, *6* (2), 104–111. https://doi.org/10.1038/nchem.1843.
18. Hong, Y. J.; Tantillo, D. J. A Potential Energy Surface Bifurcation in Terpene Biosynthesis. *Nat. Chem*. **2009**, *1* (5), 384–389. https://doi.org/10.1038/nchem.287.
19. Hong, Y. J.; Tantillo, D. J. Feasibility of Intramolecular Proton Transfers in Terpene Biosynthesis – Guiding Principles. *J. Am. Chem. Soc*. **2015**, *137* (12), 4134–4140. https://doi.org/10.1021/ja512685x.

20. Hare, S. R.; Tantillo, D. J. Post-Transition State Bifurcations Gain Momentum – Current State of the Field. *Pure Appl. Chem.* **2017**, *89* (6), 679–698. https://doi.org/10.1515/pac-2017-0104.
21. Tantillo, D. J. Chapter One - Beyond Transition State Theory – Non-Statistical Dynamic Effects for Organic Reactions. In *Advances in Physical Organic Chemistry*; Williams, I. H., Williams, N. H., Eds.; Academic Press: London, Vol. 55, 2021; pp 1–16.
22. Ess, D. H. Quasiclassical Direct Dynamics Trajectory Simulations of Organometallic Reactions. *Acc. Chem. Res*. **2021**, *54* (23), 4410–4422. https://doi.org/10.1021/acs.accounts.1c00575.
23. Lee, S.; Goodman, J. M. VRAI-Selectivity: Calculation of Selectivity beyond Transition State Theory. *Org. Biomol. Chem*. **2021**, *19* (17), 3940–3947. https://doi.org/10.1039/d1ob00234a.
24. Lee, S.; Goodman, J. M. Rapid Route-Finding for Bifurcating Organic Reactions. *J. Am. Chem. Soc*. **2020**, *142* (20), 9210–9219. https://doi.org/10.1021/jacs.9b13449.
25. Lam, C. C.; Goodman, J. M. Reaction Dynamics as the Missing Puzzle Piece: The Origin of Selectivity in Oxazaborolidinium Ion-Catalysed Reactionstle. *Chem. Sci*. **2023**, *14* (43), 12355–12365. https://doi.org/10.1039/D3SC03009A.
26. Steinfeld, J. I.; Francisco, J. S.; Hase, W. L. *Chemical Kinetics and Dynamics*, 2nd ed.; Pearson, 1998.
27. Frisch, M. J.; Trucks, G. W.; Schlegel, H. B.; Scuseria, G. E.; Robb, M. A.; Cheeseman, J. R.; Scalmani, G.; Barone, V.; Petersson, G. A.; Nakatsuji, H.; Li, X.; Caricato, M.; Marenich, A. V.; Bloino, J.; Janesko, B. G.; Gomperts, R.; Mennucci, B.; Hratchian, H. P.; Ortiz, J. V.; Izmaylov, A. F.; Sonnenberg, J. L.; Williams-Young, D.; Ding, F.; Lipparini, F.; Egidi, F.; Goings, J.; Peng, B.; Petrone, A.; Henderson, T.; Ranasinghe, D.; Zakrzewski, V. G.; Gao, J.; Rega, N.; Zheng, G.; Liang, W.; Hada, M.; Ehara, M.; Toyota, K.; Fukuda, R.; Hasegawa, J.; Ishida, M.; Nakajima, T.; Honda, Y.; Kitao, O.; Nakai, H.; Vreven, T.; Throssell, K.; Montgomery, J. A. Jr.; Peralta, J. E.; Ogliaro, F.; Bearpark, M. J.; Heyd, J. J.; Brothers, E. N.; Kudin, K. N.; Staroverov, V. N.; Keith, T. A.; Kobayashi, R.; Normand, J.; Raghavachari, K.; Rendell, A. P.; Burant, J. C.; Iyengar, S. S.; Tomasi, J.; Cossi, M.; Millam, J. M.; Klene, M.; Adamo, C.; Cammi, R.; Ochterski, J. W.; Martin, R. L.; Morokuma, K.; Farkas, O.; Foresman, J. B.; Fox, D. J. *Gaussian 16*; Gaussian, Inc.: Wallingford CT, 2016.
28. Hu, X.; Hase, W. L.; Pirraglia, T. Vectorization of the General Monte Carlo Classical Trajectory Program VENUS. *J. Comput. Chem*. **1991**, *12* (8), 1014–1024. https://doi.org/10.1002/jcc.540120814.
29. Lourderaj, U.; Sun, R.; Kohale, S. C.; Barnes, G. L.; de Jong, W. A.; Windus, T. L.; Hase, W. L. The VENUS/NWChem Software Package. Tight Coupling between Chemical Dynamics Simulations and Electronic Structure Theory. *Comput. Phys. Commun*. **2014**, *185* (3), 1074–1080. https://doi.org/10.1016/j.cpc.2013.11.011.
30. Hase, W. L.; Duchovic, R. J.; Hu, X.; Komornicki, A.; Lim, K. F.; Lu, D.; Peslherbe, G. H.; Swamy, K. N.; Linde, S. V.; Varandas, A. A. General Chemical Dynamics Computer Program. *Quantum Chem. Program Exch. Bull.* **1996**, *16*, 671.
31. Singleton, D. A.; Hang, C.; Szymanski, M. J.; Greenwald, E. E. A New Form of Kinetic Isotope Effect. Dynamic Effects on Isotopic Selectivity and Regioselectivity. *J. Am. Chem. Soc*. **2003**, *125* (5), 1176–1177. https://doi.org/10.1021/ja027221k.
32. Kwan, E. E.; Liu, R. Y. Enhancing NMR Prediction for Organic Compounds Using Molecular Dynamics. *J. Chem. Theory Comput*. **2015**, *11* (11), 5083–5089. https://doi.org/10.1021/acs.jctc.5b00856.
33. Teynor, M. S.; Wohlgemuth, N.; Carlson, L.; Huang, J.; Pugh, S. L.; Grant, B. O.; Hamilton, R. S.; Carlsen, R.; Ess, D. H. *Milo*; Brigham Young University: Provo UT, 2021.
34. Tremblay, M. T.; Yang, Z. J. The Effect of Zero-Point Energy in Simulating Organic Reactions with Post-Transition State Bifurcation. *J. Phys. Org. Chem*. **2022**, *35* (11), e4322. https://doi.org/10.1002/poc.4322.
35. Verlet, L. Computer "Experiments" on Classical Fluids. I. Thermodynamical Properties of Lennard-Jones Molecules. *Phys. Rev.* **1967**, *159* (1), 98–103. https://doi.org/10.1103/PhysRev.159.98.
36. Paranjothy, M.; Sun, R.; Zhuang, Y.; Hase, W. L. Direct Chemical Dynamics Simulations: Coupling of Classical and Quasiclassical Trajectories with Electronic Structure Theory. *WIREs Comput. Mol. Sci.* **2013**, *3* (3), 296–316. https://doi.org/10.1002/wcms.1132.
37. Senn, H. M.; Thiel, W. QM/MM Methods for Biomolecular Systems. *Angew. Chem., Int. Ed.* **2009**, *48* (7), 1198–1229. https://doi.org/10.1002/anie.200802019.
38. Acevedo, O.; Jorgensen, W. L. Advances in Quantum and Molecular Mechanical (QM/MM) Simulations for Organic and Enzymatic Reactions. *Acc. Chem. Res*. **2010**, *43* (1), 142–151. https://doi.org/10.1021/ar900171c.
39. Yang, Z.; Doubleday, C.; Houk, K. N. QM/MM Protocol for Direct Molecular Dynamics of Chemical Reactions in Solution: The Water-Accelerated Diels–Alder Reaction. *J. Chem. Theory Comput*. **2015**, *11* (12), 5606–5612. https://doi.org/10.1021/acs.jctc.5b01029.
40. Weitman, M.; Major, D. T. Challenges Posed to Bornyl Diphosphate Synthase: Diverging Reaction Mechanisms in Monoterpenes. *J. Am. Chem. Soc*. **2010**, *132* (18), 6349–6360. https://doi.org/10.1021/ja910134x.
41. Sheppard, A. N.; Acevedo, O. Multidimensional Exploration of Valley–Ridge Inflection Points on Potential-Energy Surfaces. *J. Am. Chem. Soc*. **2009**, *131* (7), 2530–2540. https://doi.org/10.1021/ja803879k.
42. Yang, Z.; Yang, S.; Yu, P.; Li, Y.; Doubleday, C.; Park, J.; Patel, A.; Jeon, B.; Russell, W. K.; Liu, H.; Russell, D. H.; Houk, K. N. Influence of Water and Enzyme SpnF on the Dynamics and Energetics of the Ambimodal [6+4]/[4+2] Cycloaddition. *Proc. Natl. Acad. Sci. U. S. A.* **2018**, *115* (5), E848–E855. https://doi.org/10.1073/pnas.1719368115.
43. Jorner, K.; Tomberg, A.; Bauer, C.; Sköld, C.; Norrby, P.-O. Organic Reactivity from Mechanism to Machine Learning. *Nat. Rev. Chem* **2021**, *5* (4), 240–255. https://doi.org/10.1038/s41570-021-00260-x.
44. Wigh, D. S.; Goodman, J. M.; Lapkin, A. A. A Review of Molecular Representation in the Age of Machine Learning. *WIREs Comput. Mol. Sci.* **2022**, *12* (5), e1603. https://doi.org/10.1002/wcms.1603.
45. Shim, E.; Tewari, A.; Cernak, T.; Zimmerman, P. M. Machine Learning Strategies for Reaction Development: Toward the Low-Data Limit. *J. Chem. Inf. Model*. **2023**, *63* (12), 3659–3668. https://doi.org/10.1021/acs.jcim.3c00577.

46. Rollins, N.; Pugh, S. L.; Maley, S. M.; Grant, B. O.; Hamilton, R. S.; Teynor, M. S.; Carlsen, R.; Jenkins, J. R.; Ess, D. H. Machine Learning Analysis of Direct Dynamics Trajectory Outcomes for Thermal Deazetization of 2,3-Diazabicyclo[2.2.1]Hept-2-Ene. *J. Phys. Chem. A* **2020**, *124* (23), 4813–4826. https://doi.org/10.1021/acs.jpca.9b10410.
47. Lyons, B. A.; Pfeifer, J.; Peterson, T. H.; Carpenter, B. K. Dynamic Models for the Thermal Deazetization of 2,3-Diazabicyclo[2.2.1]Hept-2-Ene. *J. Am. Chem. Soc*. **1993**, *115* (6), 2427–2437. https://doi.org/10.1021/ja00059a043.
48. Melville, J.; Hargis, C.; Davenport, M. T.; Hamilton, R. S.; Ess, D. H. Machine Learning Analysis of Dynamic-Dependent Bond Formation in Trajectories with Consecutive Transition States. *J. Phys. Org. Chem*. **2022**, *35* (11), e4405. https://doi.org/10.1002/poc.4405.
49. Kuan, K.-Y.; Hsu, C.-P. Predicting Selectivity with a Bifurcating Surface: Inaccurate Model or Inaccurate Statistics of Dynamics? *J. Phys. Chem. A* **2024**, *128* (32), 6798–6805. https://doi.org/10.1021/acs.jpca.4c04039.
50. Campos, R. B.; Tantillo, D. J. Designing Reactions with Post-Transition-State Bifurcations: Asynchronous Nitrene Insertions into C–C σ Bonds. *Chem* **2019**, *5* (1), 227–236. https://doi.org/10.1016/j.chempr.2018.10.019.
51. Ang, S. J.; Wang, W.; Schwalbe-Koda, D.; Axelrod, S.; Gómez-Bombarelli, R. Active Learning Accelerates Ab Initio Molecular Dynamics on Reactive Energy Surfaces. *Chem* **2021**, *7* (3), 738–751. https://doi.org/10.1016/j.chempr.2020.12.009.
52. Xue, X.-S.; Jamieson, C. S.; Garcia-Borràs, M.; Dong, X.; Yang, Z.; Houk, K. N. Ambimodal Trispericyclic Transition State and Dynamic Control of Periselectivity. *J. Am. Chem. Soc*. **2019**, *141* (3), 1217–1221. https://doi.org/10.1021/jacs.8b12674.
53. Zhou, C.; Birney, D. M. Sequential Transition States and the Valley−Ridge Inflection Point in the Formation of a Semibullvalene. *Org. Lett*. **2002**, *4* (19), 3279–3282. https://doi.org/10.1021/ol026595f.
54. Murakami, T.; Ibuki, S.; Takayanagi, T. Molecular Dynamics Simulations and Machine-Learning Assisted Study of the Reaction Path Bifurcation: Application to the Intramolecular Diels–Alder Cycloaddition between Cyclobutadiene and Butadiene. *Comput. Theor. Chem.* **2023**, *1227*, 114239. https://doi.org/10.1016/j.comptc.2023.114239.
55. Yang, Z.; Dong, X.; Yu, Y.; Yu, P.; Li, Y.; Jamieson, C.; Houk, K. N. Relationships between Product Ratios in Ambimodal Pericyclic Reactions and Bond Lengths in Transition Structures. *J. Am. Chem. Soc*. **2018**, *140* (8), 3061–3067. https://doi.org/10.1021/jacs.7b13562.
56. Bharadwaz, P.; Maldonado-Domínguez, M.; Srnec, M. Bifurcating Reactions: Distribution of Products from Energy Distribution in a Shared Reactive Mode. *Chem. Sci*. **2021**, *12* (38), 12682–12694. https://doi.org/10.1039/D1SC02826J.
57. Martin-Somer, A.; Xue, X.-S.; Jamieson, C. S.; Zou, Y.; Houk, K. N. Computational Design of a Tetrapericyclic Cycloaddition and the Nature of Potential Energy Surfaces with Multiple Bifurcations. *J. Am. Chem. Soc*. **2023**, *145* (7), 4221–4230. https://doi.org/10.1021/jacs.2c12871.
58. Shin, W.; Hou, Y.; Wang, X.; Yang, Z. J. Interplay between Energy and Entropy Mediates Ambimodal Selectivity of Cycloadditions. *J. Chem. Theory Comput*. **2024**, *20* (24), 10942–10951. https://doi.org/10.1021/acs.jctc.4c01138.
59. Becke, A. D. Density-functional Thermochemistry. III. The Role of Exact Exchange. *J. Chem. Phys*. **1993**, *98* (7), 5648–5652. https://doi.org/10.1063/1.464913.
60. Lee, C.; Yang, W.; Parr, R. G. Development of the Colle-Salvetti Correlation-Energy Formula into a Functional of the Electron Density. *Phys. Rev. B* **1988**, *37* (2), 785–789. https://doi.org/10.1103/PhysRevB.37.785.
61. Becke, A. D. Density-Functional Exchange-Energy Approximation with Correct Asymptotic Behavior. *Phys. Rev. A (Coll Park)* **1988**, *38* (6), 3098–3100. https://doi.org/10.1103/PhysRevA.38.3098.
62. Lam, C. C.; Goodman, J. M. CONFPASS: Fast DFT Re-Optimizations of Structures from Confor-Mation Searches. *J. Chem. Inf. Model*. **2023**, *63* (14), 4364–4375. https://doi.org/10.1021/acs.jcim.3c00649.
63. Zhang, Y.; Cao, C.; She, Y.; Davies, H. M. L.; Yang, Y.-F.; Houk, K. N. Molecular Dynamics of the Davies Ambimodal C–H Functionalization/Cope Rearrangement Reaction. *J. Org. Chem*. **2024**, *89* (23), 17176–17186. https://doi.org/10.1021/acs.joc.4c01682.

Supplementary Material: This article contains supplementary material (https://doi.org/10.1515/pac-2025-0462).